

Green Chemistry

Accepted Manuscript



This article can be cited before page numbers have been issued, to do this please use: F. Liu, Q. Liu, J. Xu, L. Li, Y. Cui, R. Lang, L. Li, Y. Su, S. Miao, H. Sun, B. Qiao, A. Wang, F. Jerome and T. Zhang, *Green Chem.*, 2018, DOI: 10.1039/C8GC00039E.



This is an Accepted Manuscript, which has been through the Royal Society of Chemistry peer review process and has been accepted for publication.

Accepted Manuscripts are published online shortly after acceptance, before technical editing, formatting and proof reading. Using this free service, authors can make their results available to the community, in citable form, before we publish the edited article. We will replace this Accepted Manuscript with the edited and formatted Advance Article as soon as it is available.

You can find more information about Accepted Manuscripts in the [author guidelines](#).

Please note that technical editing may introduce minor changes to the text and/or graphics, which may alter content. The journal's standard [Terms & Conditions](#) and the ethical guidelines, outlined in our [author and reviewer resource centre](#), still apply. In no event shall the Royal Society of Chemistry be held responsible for any errors or omissions in this Accepted Manuscript or any consequences arising from the use of any information it contains.



Journal Name

ARTICLE

Catalytic cascade conversion of furfural to 1,4-pentanediol in a single reactor

Fei Liu,[†] Qiaoyun Liu,[†] Jinming Xu,^a Lei Li,^c Yi-Tao Cui,^d Rui Lang,^a Lin Li,^a Yang Su,^a Shu Miao,^a Hui Sun,^a Botao Qiao,^{*a} Ai Qin Wang,^{*a} Francois Jerome^{*e} and Tao Zhang^a

Received 00th January 20xx,
Accepted 00th January 20xx

DOI: 10.1039/x0xx00000x

www.rsc.org/

The synthesis of bio-based linear diols is the subject of many researches. However, one of the main obstacles in industrial development is the difficulty in controlling the product selectivity. Here, we report the catalytic conversion of furfural to 1,4-pentanediol (PD) in the presence of Ru supported on an ordered mesoporous carbon (CMK-3) under pressure of H₂ and CO₂ in water. In contrast to previous catalytic pathways, this work is distinct in that it yields 1,4-PD as an exclusive product, instead of a mixture of 1,2- and 1,5-PD as usual. Under optimized conditions, 1,4-PD was produced in 90% yield, and in a one-pot reaction, directly from furfural. We disclose that the conversion of furfural to 1,4-PD followed a unusual catalytic route. It implies a bifunctional catalytic pathway based on sequential catalytic hydrogenation reactions and an acid-catalyzed Piancatelli's rearrangement.

Introduction

Linear diols are of utmost importance in chemistry and find nowadays many applications in our society. In particular, diols are widely employed as solvent in cosmetic industry.¹ They also serve as intermediates in the manufacture of fine/specialty chemicals, as monomers in the fabrication of polymers and as polar head in the synthesis of biosurfactants.² To date, linear diols are produced on an industrial scale from fossil-based resources. The rapid emergence of plant-based industry is now opening opportunities to produce bio-based linear diols, often with a similar chemical structure to diols from a fossil origin, but with a much improved carbon footprint.³⁻⁷ Among the different strategies previously reported, the synthesis of bio-based pentanediol (PD) from industrially available furfural has attracted particular interest.⁸⁻¹⁰ To date, current catalytic strategies involves the hydrogenolysis of the C-O bond of the furanic ring in the presence of a metal-based catalyst.¹¹⁻¹⁴ This catalytic pathway takes place at relatively high temperatures (100-170 °C) and pressures of H₂ (3-6 MPa). Under these harsh reaction conditions, over-hydrogenation/hydrogenolysis reaction also

occurs to a more or less extent depending on the catalyst. On the other hand, these catalytic routes afford mainly 1,2 and 1,5-PD, often as a mixture of both, in a 50-80% yield (1,2 + 1,5-PD) (Figure 1). As a general trend, metals on basic supports such as Pt/HT¹², Cu/LDO¹⁵ and Pt/CeO₂¹⁶ afford mainly 1,2-PD while metals on acid supports such as Pd-Ir-ReO_x/SiO₂¹⁴ and Rh-Ir-ReO_x/SiO₂¹⁷ are more selective to 1,5-PD (Table S1). So far, none of these catalysts are able to produce selectively 1,4-PD. For instance, only a maximum yield of 30% in 1,4-PD was claimed from furfural over a Pd-Ir-ReO_x/SiO₂ bifunctional catalyst.¹⁴ In contrast to 1,2- and 1,5-PD, 1,4-PD is currently not produced (industrially speaking) from fossil oils which open business opportunities in term of product development. At a lab scale, 1,4-PD and its precursor (3-acetyl-1-propanol, 3-AP) were reported as valuable organic building blocks, in particular in the synthesis of chloroquine, one of the most effective medicines for both prevention and treatment of malaria.¹⁸ Switching the selectivity of the current catalytic processes from 1,2/1,5-PD to 1,4-PD is not an easy task and it requires searching novel catalytic pathways. 1,4-PD was previously synthesized through catalytic hydrogenation of levulinic acid (LA) or γ -valerolactone at 80-200 °C and under 6-15 MPa of H₂ in the presence of metal catalysts such as Ru, Pt/Mo, Rh/Mo and Cu, to mention a few.¹⁹⁻²³ Although moderate to good yields (70-96%) were claimed, the availability and/or the current price of levulinic acid or γ -valerolactone are still important limitations for such application.

Finding innovative catalytic routes capable of converting selectively furfural to 1,4-PD in a one pot process would definitely increase the attractiveness of the furfural platform for the supply of bio-based PD. To reach this objective, two criteria should be fulfilled: (1) identifying a novel reaction

^a State Key Laboratory of Catalysis, Dalian Institute of Chemical Physics, Chinese Academy of Sciences, Dalian, 116023, PR China. E-mail: bqiao@dicp.ac.cn, aqwang@dicp.ac.cn

^b University of Chinese Academy of Sciences, Beijing, 100049, PR China

^c Synchrotron Radiation Nanotechnology Center, University of Hyogo, Hyogo 679-5165, Japan.

^d Institute for Solid State Physics, The University of Tokyo, Hyogo 679-5198, Japan.

^e Institut de Chimie des Milieux et Matériaux de Poitiers, CNRS/University of Poitiers, Poitiers 86073, France. E-mail: francois.jerome@univ-poitiers.fr

[†] Electronic Supplementary Information (ESI) available: [details of any supplementary information available should be included here]. See DOI: 10.1039/x0xx00000x

*These authors contributed equally.

pathway to switch the selectivity of the reaction from 1,2/1,5-PD to 1,4-PD and (2) designing solid catalysts able to promote this reaction under mild conditions to prevent over-hydrogenation/hydrogenolysis reactions of PD or furfural.

This work addresses this issue and we disclose here a catalytic pathway capable of selectively converting furfural in a one pot process to 1,4-PD in the presence of Ru supported on an ordered mesoporous carbon so-called CMK-3 (Figure. 1). This catalytic route involves a series of cascade hydrogenation and acid-catalyzed reactions. Hydrogenation reactions were catalyzed by Ru nanoparticles while acid sites stemmed either from the CMK-3 support or the acidification of water with CO₂ as previously reported.²⁴ Thanks to the mild reaction conditions (60-80 °C and 1 MPa H₂), 1,4-PD is selectively obtained in yield up to 90%. To the best of our knowledge, this work constitutes an important advance in the field by opening the first selective access to 1,4-PD from furfural.

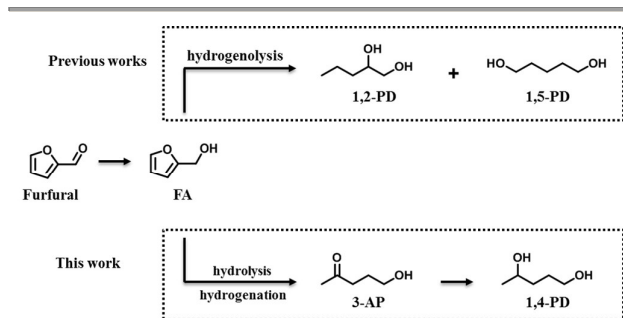


Figure 1. Originality of this work.

Results and discussion

The ordered mesoporous carbon (CMK-3) support was synthesized by a hard-templating method using 2D hexagonal SBA-15 as an inorganic template, as described previously.²⁵ More information on the synthesis of CMK-3 is provided in the SI. The Ru species were introduced on the CMK-3 by an impregnation method with an actual Ru loading of 2 wt%. The sample was treated thermally at 300 °C in N₂ flow for 3 h yielding the so-called Ru/CMK-3-unred. The Ru/CMK-3-unred catalyst was then subjected to a temperature programmed reduction (TPR) treatment under 10% H₂/He gas from ambient temperature to 200 and 400 °C, and denoted hereafter Ru/CMK-3-R200 and Ru/CMK-3-R400, respectively.

The X-ray diffraction (XRD) patterns of pure CMK-3 and Ru/CMK-3 catalysts showed that all samples presented only two broad peaks at around 23° and 43° which were ascribed to the amorphous carbon (Figure S1)²⁶. It should be noted that no Ru diffraction peak was observed on all Ru/CMK-3 samples, suggesting that Ru species are highly dispersed on the support. To verify this, high-angle annular dark-field (HAADF) scanning transmission electron microscopy (STEM) was further used to characterize the Ru species. Typical HAADF-STEM images show that Ru nanoparticles are uniformly dispersed on the CMK-3 support, and the particle size distribution depends on the pretreatment conditions (Figure 2, and more images see Figure

S2 and S3). For the un-reduced Ru/CMK-3 catalyst, the average particle size is 0.9 nm, while it is 1.0 nm for the Ru/CMK-3-R200 and 3.8 nm for the Ru/CMK-3-R400, indicating that the reduction at mild conditions (*e.g.*, 200 °C) does not cause the obvious growing of Ru nanoparticles while a higher reduction temperature (*e.g.*, 400 °C) leads to agglomeration of Ru nanoparticles.

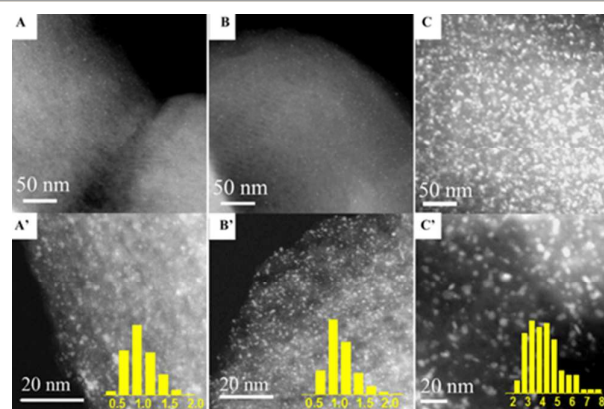


Figure 2. HAADF-STEM images of Ru/CMK-3-unred (A, A'), Ru/CMK-3-R200 (B, B') and Ru/CMK-3-R400 (C, C') and the corresponding size distributions.

The oxidation states of Ru species were probed by X-ray absorption spectroscopy as it is sensitive to both the chemical state and the local structure of the measured metals. Considering that the reduced Ru species might be easily re-oxidized upon exposure to air, we performed an *in situ* measurement. The reduction procedure is slightly different from that for the TPR treatment. In this condition, a 5% H₂/He was used and the samples were reduced for 20 min at each temperature (for more details, see supporting information). The near edge (XANES) presented in Figure S4 suggest that the Ru species on the un-reduced Ru/CMK-3 sample exist in an oxidation state lower than +4 since the edge is lower than that of RuO₂. After reduction at 200 °C, the Ru species were slightly reduced but still in a positively charged state. However, with reduction at 400 °C, Ru was almost completely reduced to metallic state as its edge almost coincides with that of the Ru foil. A quick fitting of the spectra further confirmed this conclusion (Table S2). In Ru/CMK-3-unred sample, besides Ru-Ru bond, there are Ru-Cl and Ru-O bonds which should originate from the RuCl₃ precursor and the interaction of Ru with O-containing group on the CMK-3, respectively. In Ru/CMK-3-R200 sample, Ru-Cl bonds are still observed while the Ru-O bond disappeared, consistent with a partial reduction of Ru. In Ru/CMK-3-R400 catalyst, only Ru-Ru bond was found, suggesting that Ru was fully reduced to form metallic Ru, in line with the near edge results. In addition, on Ru/CMK-3-R400 sample, the coordination number of Ru-Ru was fitted to be 10.2. Considering that Ru has a very similar atomic radius to Pt, it could be roughly calculated, based on the coordination number according to a previous report,²⁷ that the size of Ru

NPs is about 3 nm. This value agrees well with the STEM results described above.

The acid sites of the catalysts were probed with NH_3 -TPD experiments and the results are shown in Figure S5 and Table S3. The acid density varies with the reduction temperature, and the Ru/CMK-3-R200 has the maximum acid density (425 $\mu\text{mol/g}$), followed with Ru/CMK-3-unred (271 $\mu\text{mol/g}$) and Ru/CMK-3-R400 (205 $\mu\text{mol/g}$). In contrast, the blank CMK-3 support has the lowest acid density (61 $\mu\text{mol/g}$), indicating that the acidity stems mainly from Ru species.²⁸ Comparing the trend of acid density with that of Ru valence state, we can conclude

that the acidity arises mainly from the positively charged Ru species, which is in accordance with the previous reports.²⁸ The NH_3 -TPD profiles (Figure S5) show that both Ru/CMK-3-unred and Ru/CMK-3-R200 contain primarily weak acid sites.

In a first set of experiments, furfural was hydrogenated in water in the presence of the Ru/CMK-3-R200 catalyst (0.57 mol% of Ru). Results are summarized in Table 1. At 80 °C and a pressure of H_2 of 1 MPa, furfural was consumed completely after 20 h of reaction (entry 1). Unexpectedly, 1,4-PD was formed as the major product (61 % yield), suggesting that this catalytic process did not occur through a classical hydrogenolysis mechanism. The only other detectable product was THFA (17% yield), resulting from the over-hydrogenation of furfural. The 22% unidentified carbon revealed that side reactions concomitantly took place. When the H_2 pressure was increased to 4 MPa, the yield to 1,4-PD remained unchanged. However, under these conditions, THFA was formed in 35% yield (entry 2), and only less than 5% of unknown products were formed. To our delight, when the reactor was pressurized with 2 MPa of CO_2 and 2 MPa of H_2 (total pressure of 4 MPa), the yield to 1,4-PD was increased to 71% and further to 90%

when the partial pressures of CO_2 and H_2 were adjusted to 3 MPa and 1 MPa, respectively (entry 3-4). This result suggests that the acidification of the reaction media (*in situ* formation of carbonic acid) had a positive effect on the selectivity to 1,4-PD. Interestingly, when the partial pressure of CO_2 was further increased (CO_2/H_2 : 3.5/0.5 MPa), the conversion of furfural dropped down to 82% and the yield of 1,4-PD went down to 57% (entry 5). Furthermore, without H_2 , no 1,4-PD was formed, indicating that the direct conversion of furfural to 1,4-PD presumably followed a bifunctional acid/hydrogenation catalytic route. More information on the reaction mechanism is provided below. It is worth noting that compared to the best results reported so far for the production of 1,2- and 1,5-PD from furfural (Table S1) and even 1,4-PD from LA (Table S4), the 1,4-PD yields obtained in this work are among the best ones, essentially thanks to the mildest conditions of pressures and temperatures.

The mesopores plays an important role on the activity and selectivity of Ru/CMK-3-R200. When SBA-15 (template) was removed during the preparation of the catalyst, Ru dispersed over a microporous carbon was obtained and denoted hereafter Ru/C. In the presence of this Ru/C, no 1,4-PD was produced (Table 1, entry 6). Instead, FA (26% yield), THFA (11% yield), 3-AP (10% yield) and 20% of unidentified chemicals were observed. The lower BET surface and the lower amount of acid sites (91 $\mu\text{mol/g}$) on Ru/C may explain this difference of catalytic performances with Ru/CMK-3-R200 (supporting information).

To collect more information on the role of Ru, the un-reduced Ru/CMK-3 and the Ru/CMK-3-R400 were also tested under the optimized conditions (entries 7 and 8). Evidently, the un-reduced Ru/CMK-3 influences negatively the rate of the hydrogenation step and in this case, acid-catalyzed reaction

Table 1. Optimization of the reaction parameters over Ru/CMK-3 catalyst.^[a]

The reaction scheme shows furfural (a furan ring with an aldehyde group) reacting with H_2/CO_2 over a Ru/CMK-3 catalyst. The products are 1,4-PD (1,4-pentanediol), THFA (2-thiofuranol), FA (furfural alcohol), and 3-AP (3-aminopropan-1-ol).

Entry	Catalyst	CO_2/H_2 (MPa/MPa)	Conv. (%)	1,4-PD Yield (%)	THFA Yield (%)	FA Yield (%)	3-AP Yield (%)	Others Yield (%) ^b	Productivity ^d ($\text{mol}^{-1} \cdot \text{g}_{\text{Ru}}^{-1} \cdot \text{h}^{-1}$) $\times 10^2$
1	Ru/CMK-3-R200	0/1	100	61	17	0	0	22	5.3
2	Ru/CMK-3-R200	0/4	100	61	34	0	0	5	5.3
3	Ru/CMK-3-R200	2/2	100	71	18	4	0	7	6.2
4	Ru/CMK-3-R200	3/1	100	90	9	0	0	1	7.8
5	Ru/CMK-3-R200	3.5/0.5	82	57	8	0	15	2	4.1
6	Ru/C	3/1	67	0	11	26	10	20	0
7	Ru/CMK-3-unred	3/1	100	75	10	0	0	15	6.5
8	Ru/CMK-3-R400	3/1	100	35	15	0	0	50	3.0
9 ^c	Ru/CMK-3-R400	3/1	100	6	35	0	41	18	0.5

[a] Reaction conditions: 2 wt% furfural in H_2O , 5 mL H_2O , 20 h and a metal/substrate ratio of 0.57 mol% at 80 °C; [b] others products stem either from over-hydrogenation reactions (C-C bond cracking) or acid-catalyzed degradation of intermediates leading to the formation of oligomeric and tar-like products; [c] at 60 °C; [d] Productivities (mol product per g of Ru and per hour).

occurred dominantly leading to the conversion of furfural to undesirable side products; the yield in 1,4-PD dropped from 90 to 75% (entry 7). As can be seen in Figure S6, Ru/CMK-3-R200 and Ru/CMK-3-R400 exhibited a similar activity (97% conversion vs 92% after 5 hours of reaction for Ru/CMK-3-R200 and Ru/CMK-3-R400, respectively). However, Ru/CMK-3-R200 was significantly more selective into 3-AP and 1,4-PD than Ru/CMK-3-R400, this latter favoring overhydrogenation/hydrogenolysis reactions. Lowering the reaction temperature to 60 °C partly inhibited overhydrogenation/hydrogenolysis reactions with Ru/CMK-3-R400, but the yield to 1,4-PD remained as low as 6% (entry 8). This result suggested that Ru/CMK-3-R400 catalyst has a higher H₂ activation ability than Ru/CMK-3-R200 which is partly reduced only. In order to verify this claim, a microcalorimetric measurement of H₂ adsorption was carried out.²⁹ Amount of adsorbed H₂ on both samples were small, *i.e.*, ~2 μmol·g⁻¹ on Ru/CMK-3-R200 and ~10 μmol·g⁻¹ on Ru/CMK-3-R400, respectively. However, the adsorption strength was totally different: initial adsorption heat on Ru/CMK-3-R200 was about 30 kJ·mol⁻¹ whereas on Ru/CMK-3-R400 a value of about 70 kJ·mol⁻¹ was determined which is similar to the adsorption heat on Pd/C catalyst.³⁰ These results demonstrated that Ru/CMK-3-R200 is less active for H₂ activation than Ru/CMK-3-R400 and this moderate H₂ activation ability is crucial to achieve high selectivity into 1,4-PD. The difference in the capability for H₂ activation is closely associated with the electronic property of Ru. The valence state of Ru decreases in the order of Ru/CMK-3-unred > Ru/CMK-3-R200 > Ru/CMK-3-R400 (Figure S4), which is in reverse order with the initial adsorption heat of H₂, indicating that metallic Ru⁰ is responsible for hydrogenation.

The recyclability of the Ru-CMK-3-R200 did not reveal any decrease of its catalytic activity cycle after cycle. However, the selectivity to 1,4-PD started decreasing after 3 catalytic cycles (Figure S7), suggesting a change in the catalyst chemical composition. A hot filtration test revealed that it was a truly heterogeneously-catalyzed process meaning that a proper reactivation of the Ru-CMK-3-R200 will be thus required for long term recycling.

To elucidate this unexpected reaction pathway observed with Ru/CMK-3-R200, the temperature of the reaction was varied (Figure 3). In agreement with the Arrhenius's law, the temperature has an important effect on the reaction progress. At 100 °C (CO₂/H₂: 3/1 MPa), THFA was formed in a higher proportion due to the enhanced hydrogenation ability of Ru/CMK-3-R200 at this temperature. In contrast, at 60 °C, 3-AP was formed as a dominant product (73% yield, and even 84% at prolonged reaction time) while at 40 °C, FA was observed as the main product (70%). Note that the 3-AP yield obtained at 60 °C is comparable to or even better than those reported from previous works involving bacteria or homogenous catalysts (Table S5) using LA, alkynes and even 1,4-PD as a starting material.³¹⁻³⁶ Altogether, these results suggest that the catalytic conversion of furfural to 1,4-PD involves a cascade of reactions with FA and 3-AP being two important intermediates.

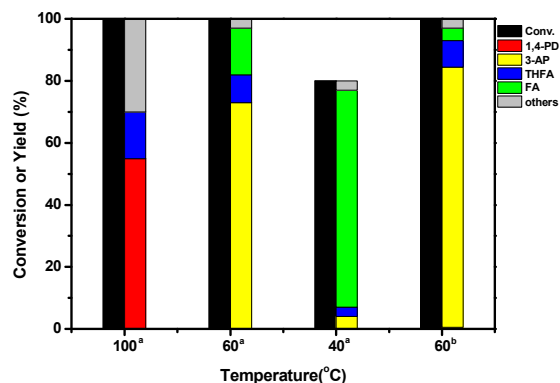


Figure 3. Effects of reaction temperature on the conversion of furfural and the yields of products in the presence of Ru/CMK-3-R200. [a] Reaction conditions: 2 wt% furfural in H₂O, 5 mL H₂O, 20 h and a metal/substrate ratio of 0.57 mol%. [b] Reaction time 30 h.

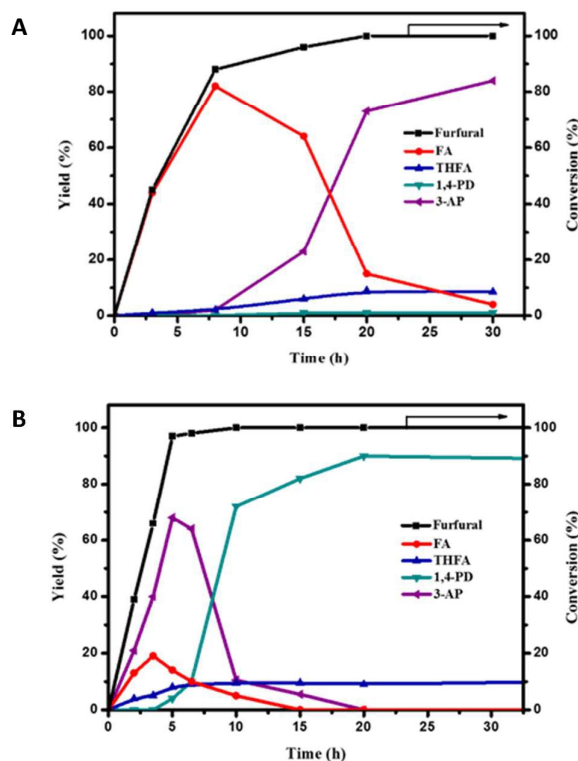


Figure 4. Kinetic time course of the furfural transformation in the presence of Ru/CMK-3-R200 at 60 °C (A) and 80 °C (B). Reaction condition: furfural (0.1g), H₂O (5 mL), CO₂/H₂: 3MPa/1MPa, a metal/substrate ratio of 0.57 mol%.

To support this claim, we plotted the yield of FA, 3-AP and 1,4-PD versus time at both 80 °C and 60 °C (Figure 4). At 60 °C, FA was selectively formed with 82% yield up to 8 hours of reaction. At prolonged reaction time, the FA yield decreased gradually with a concomitant increase of the 3-AP yield up to

84% at 30 hours accompanied with the formation of a small amount of THFA and a negligible 1,4-PD generation. At 80 °C, the conversion of furfural reached 90% after 5 hours of reaction. Main products were in this case FA and 3-AP, accompanied by a small amount of THFA and 1,4-PD (Figure 3b). At prolonged reaction time, both FA and 3-AP were consumed and the yield of 1,4-PD increased gradually to reach a maximum of 90% after 20 h of reaction. These kinetic profiles revealed clearly that the catalytic process involves the following sequence (1) a hydrogenation of furfural to FA followed by (2) the conversion of FA to 3-AP and then (3) hydrogenation of 3-AP to 1,4-PD.

In aqueous acidic media, it is generally believed that FA can react with water to form LA.³⁷ Therefore, one possible route is the conversion of FA to LA, LA to 3-AP and finally 3-AP to 1,4-PD. However, in the kinetic profiles presented in Figures 3 and 4, no LA was detected, suggesting that in our reaction conditions either LA was not an intermediate or its *in situ* hydrogenation to 3-AP was quasi instantaneous. To check this possibility, we then performed the reduction of LA in the identical optimized conditions reported in Table 1, entry 4. To our surprise, neither 3-AP nor 1,4-PD were generated, and instead LA was converted to γ -valerolactone in 95% yield (Figure S8A). A control experiment under identical experimental conditions but with γ -valerolactone as the starting material was further carried out and the result showed also that no conversion occurred at all within a 20-hour test (Figure S8B). This result is consistent with published reports which have indicated that the hydrogenation of γ -valerolactone over Ru-based solid catalysts required harsher conditions of pressure and temperature than ours.³⁸

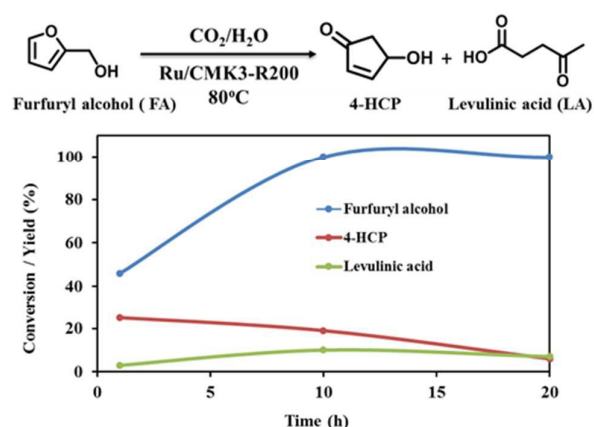


Figure 5. Kinetic time course of the FA conversion in $\text{CO}_2/\text{H}_2\text{O}$ system at 80 °C in the absence of hydrogen.

Next, the reaction was examined from FA in the presence of the Ru/CMK-3-R200 catalyst under the same reaction conditions but in the absence of H_2 . As shown in the kinetic profile presented in Figure 5, under these conditions, 4-hydroxy-2-cyclopentenone (4-HCP) was formed with ~25% yield after 1h of reaction. LA was concomitantly formed but at a much lower rate. Other products were soluble and insoluble

tar-like materials such as humins and/or oligomers of FA. 4-HCP can be obtained through the Piancatelli rearrangement of FA. In contrast to the conversion of FA to LA that typically occurs in the presence of strong acid sites, the Piancatelli rearrangement of FA is generally favored by the presence of weak acid sites.³⁹⁻⁴¹ In good agreement, when the reaction was conducted under $\text{CO}_2/\text{H}_2\text{O}$ in the absence of Ru/CMK-3-R200 catalyst, 4-HCP was still produced as a major product, although at a different rate. From a catalytic point of view, this result indicates that Ru/CMK-3-R200 exhibit weak acid sites, otherwise LA would have been produced as a major product. In our case, the weak acid sites required for the reaction are thus provided by both the positively charged Ru species and the water-dissolved CO_2 .

From all these results, a plausible reaction pathway may be proposed to explain this unexpected and selective conversion of furfural to 1,4-PD instead of 1,2- or 1,5-PD as usual. The first step is the hydrogenation of furfural to FA. Then, FA underwent a Piancatelli rearrangement catalyzed by weak acids present on Ru/CMK-3-R200 or generated by dissolving CO_2 into water (*in situ* production of carbonic acid). The overall Piancatelli transformation is believed to proceed through a cascade sequence that terminates with a 4π electrocyclic ring closure of a pentadienyl cation, as shown in Figure S9. Under our reaction conditions, we propose that the pentadienyl cation was trapped *in situ* by hydrogenation over Ru/CMK-3, yielding 3-AP and then 1,4-PD. This reaction pathway is displayed in figure 6.

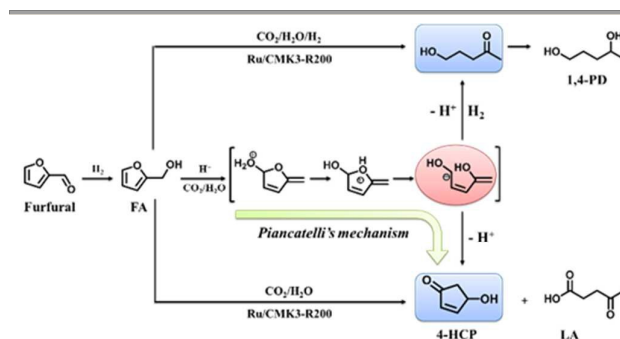


Figure 6. Proposed mechanism for 1,4-PD synthesis in the dual acid/hydrogenation catalytic system.

Conclusions

We demonstrate that the hydrogenation of furfural at 80 °C over Ru/CMK-3-R200 in water and under a CO_2/H_2 pressure permitted an access to 1,4-PD in yield up to 90%. This catalytic route is distinct from previous strategies in that it exclusively affords 1,4-PD instead of a mixture of 1,2- and 1,5-PD as usual. In addition, the mild conditions of pressure and temperature required in our strategy suppresses unwanted over-hydrogenation/hydrogenolysis reactions which is often an important limitation of the current catalytic processes converting furfural to 1,2/1,5-PD. We discovered that the conversion of furfural to 1,4-PD followed a catalytic pathway unreported to date. It implies a bifunctional catalytic pathway: (1) a

ARTICLE

Journal Name

catalytic hydrogenation of furfural to FA follows by (2) an acid-catalyzed Piancatelli-type rearrangement yielding 3-AP, after in situ hydrogenation of the pentadienyl cation intermediate, and finally (3) a hydrogenation of 3-AP to 1,4-PD. In our conditions, the Piancatelli rearrangement of FA was favored by the presence of weak acid sites which are provided by the positively charged Ru species and the water-dissolved pressurized CO₂. Importantly, by lowering the temperature of the reaction to 60 °C, it was even possible to selectively stop the reaction at the 3-AP product, another valuable chemical. It is noteworthy that a further drop of the temperature to 40 °C may also be a selective mean to synthesize furfuryl alcohol, highlighting that the selectivity of this reaction can be easily tuned. To the best of our knowledge, this work constitutes an important advance in the field by opening a one-pot and selective access to 1,4-PD (or 3-AP) from furfural, thus definitely increasing the attractiveness of the furfural platform for the supply of bio-based PD.

Conflicts of interest

There are no conflicts to declare.

Acknowledgements

This work was supported by National Natural Science Foundation of China (21606227, 21690080-21690084, 21673228, 21776270), Strategic Priority Research Program of the Chinese Academy of Sciences (XDB17020100), National Key Projects for Fundamental Re-search and Development of China (2016YFA0202801). Department of science and technology of Liaoning province (2015020086-101). The synchrotron radiation experiment was performed at the 1W1B beamline of the Beijing Synchrotron Radiation Facility (BSRF) operated at 200 mA and 2.2 GeV, and the BL08B2 of SPring-8 with the approval of Japan Synchrotron Radiation Research Institute (Proposal No. 2017A3302).

Notes and references

1. A. A. Koutinas, A. Vlysidis, D. Pleissner, N. Kopsahelis, I. Lopez Garcia, I. K. Kookos, S. Papanikolaou, T. H. Kwan and C. S. K. Lin, *Chem. Soc. Rev.*, 2014, **43**, 2587-2627.
2. P. Werle, M. Morawietz, S. Lundmark, K. Sørensen, E. Karvinen and J. Lehtonen, *In Ullman's Fine Chemicals; Elvers, B., Ed. Wiley-VCH: Weinheim, Germany*, 2014, **Vol. 1**, 37-58.
3. T. Buntara, S. Noel, P. H. Phua, I. Melián-Cabrera, J. G. de Vries and H. J. Heeres, *Angew. Chem. Int. Ed.*, 2011, **50**, 7083-7087.
4. N. Ji, T. Zhang, M. Zheng, A. Wang, H. Wang, X. Wang and J. G. Chen, *Angew. Chem. Int. Ed.*, 2008, **47**, 8510-8513.
5. K. Chen, S. Koso, T. Kubota, Y. Nakagawa and K. Tomishige, *ChemCatChem*, 2010, **2**, 547-555.
6. M. Chia, Y. J. Pagán-Torres, D. Hibbitts, Q. Tan, H. N. Pham, A. K. Datye, M. Neurock, R. J. Davis and J. A. Dumesic, *J. Am. Chem. Soc.*, 2011, **133**, 12675-12689.
7. M. Zheng, J. Pang, A. Wang, T. Zhang, *Chin. J. Catal.*, 2014, **35**, 602-613.
8. J.-P. Lange, E. van der Heide, J. van Buijtenen and R. Price, *ChemSusChem*, 2012, **5**, 150-166.
9. R. Mariscal, P. Maireles-Torres, M. Ojeda, I. Sadaba and M. Lopez Granados, *Energy & Environ. Sci.*, 2016, **9**, 1144-1189.
10. L. T. Mika, E. Cséfalvay and Á. Németh, *Chem. Rev.*, 2018, **118**, 505-613.
11. Y. Nakagawa, M. Tamura and K. Tomishige, *Catalysis Surveys from Asia*, 2015, **19**, 249-256.
12. T. Mizugaki, T. Yamakawa, Y. Nagatsu, Z. Maeno, T. Mitsudome, K. Jitsukawa and K. Kaneda, *ACS Sus. Chem. Eng.*, 2014, **2**, 2243-2247.
13. S. Liu, Y. Amada, M. Tamura, Y. Nakagawa and K. Tomishige, *Catal. Sci. Technol.*, 2014, **4**, 2535-2549.
14. S. Liu, Y. Amada, M. Tamura, Y. Nakagawa and K. Tomishige, *Green Chem.*, 2014, **16**, 617-626.
15. H. Liu, Z. Huang, F. Zhao, F. Cui, X. Li, C. Xia and J. Chen, *Catal. Sci. Technol.*, 2016, **6**, 668-671.
16. R. Ma, X.-P. Wu, T. Tong, Z.-J. Shao, Y. Wang, X. Liu, Q. Xia and X.-Q. Gong, *ACS Catal.*, 2017, **7**, 333-337.
17. S. Koso, H. Watanabe, K. Okumura, Y. Nakagawa and K. Tomishige, *Appl. Catal. B*, 2012, **111-112**, 27-37.
18. T. Lei, Z. Chi and L. Jian, *J. Chem. Pharm. Res.*, 2013, **5**, 396-401.
19. L. Corbel-Demilly, B.-K. Ly, D.-P. Minh, B. Tapin, C. Espécel, F. Epron, A. Cabiacc, E. Guillon, M. Besson and C. Pinel, *ChemSusChem*, 2013, **6**, 2388-2395.
20. T. Mizugaki, Y. Nagatsu, K. Togo, Z. Maeno, T. Mitsudome, K. Jitsukawa and K. Kaneda, *Green Chem.*, 2015, **17**, 5136-5139.
21. M. Li, G. Li, N. Li, A. Wang, W. Dong, X. Wang and Y. Cong, *Chem. Commun.*, 2014, **50**, 1414-1416.
22. X.-L. Du, Q.-Y. Bi, Y.-M. Liu, Y. Cao, H.-Y. He and K.-N. Fan, *Green Chem.*, 2012, **14**, 935-939.
23. H. Mehdi, V. Fábos, R. Tuba, A. Bodor, L. T. Mika and I. T. Horváth, *Topics in Catalysis*, 2008, **48**, 49-54.
24. F. Liu, M. Audemar, K. D. O. Vigier, J.-M. Clacens, F. De Campo and F. Jerome, *ChemSusChem*, 2014, **7**, 2089-2093.
25. G. Xu, A. Wang, J. Pang, X. Zhao, J. Xu, N. Lei, J. Wang, M. Zheng, J. Yin and T. Zhang, *ChemSusChem*, 2017, **10**, 1390-1394.
26. T. Komanoya, H. Kobayashi, K. Hara, W.-J. Chun and A. Fukuoka, *Appl. Catal. A*, 2011, **407**, 188-194.
27. A. Jentys, *Phys. Chem. Chem. Phys.*, 1999, **1**, 4059-4063.
28. G. Liang, A. Wang, L. Li, G. Xu, N. Yan and T. Zhang, *Angew. Chem. Int. Ed.*, 2017, **56**, 3050-3054.
29. L. Li, J. Lin, X. Li, A. Wang, X. Wang and T. Zhang, *Chin. J. Catal.*, 2016, **37**, 2039-2052.
30. B. Qiao, J. Lin, L. Li, A. Wang, J. Liu and T. Zhang, *ChemCatChem*, 2014, **6**, 547-554.
31. Y. Ni, P.-L. Hagedoorn, J.-H. Xu, I. W. C. E. Arends and F. Hollmann, *Chem. Commun.*, 2012, **48**, 12056-12058.
32. M. Gatto, P. Belanzoni, L. Belpassi, L. Biasiolo, A. Del Zotto, F. Tarantelli and D. Zuccaccia, *ACS Catal.*, 2016, **6**, 7363-7376.
33. E. A. Baquero, G. F. Silbestri, P. Gómez-Sal, J. C. Flores and E. de Jesús, *Organometallics*, 2013, **32**, 2814-2826.
34. Y. Ishii, T. Yoshida, K. Yamawaki and M. Ogawa, *The Journal of Organic Chemistry*, 1988, **53**, 5549-5552.

Journal Name

ARTICLE

35. H. M. Jung, J. H. Choi, S. O. Lee, Y. H. Kim, J. H. Park and J. Park, *Organometallics*, 2002, **21**, 5674-5677.
36. J. Wang, L. Yan, G. Qian, S. Li, K. Yang, H. Liu and X. Wang, *Tetrahedron*, 2007, **63**, 1826-1832.
37. P. Azadi, R. Carrasquillo-Flores, Y. J. Pagan-Torres, E. I. Gurbuz, R. Farnood and J. A. Dumesic, *Green Chem.*, 2012, **14**, 1573-1576.
38. W. Cao, W. Luo, H. Ge, Y. Su, A. Wang and T. Zhang, *Green Chem.*, 2017, **19**, 2201-2211.
39. M. Hronec, K. Fulajtárová and T. Soták, *Journal of Industrial and Engineering Chemistry*, 2014, **20**, 650-655.
40. G. Piancatelli, A. Scettri and S. Barbadoro, *Tetrahedron Lett.*, 1976, **17**, 3555-3558.
41. G. Piancatelli, M. D'Auria and F. D'Onofrio, *Synthesis*, 1994, **1994**, 867-889.